Shear Bands in Glassy Amorphous Polymers

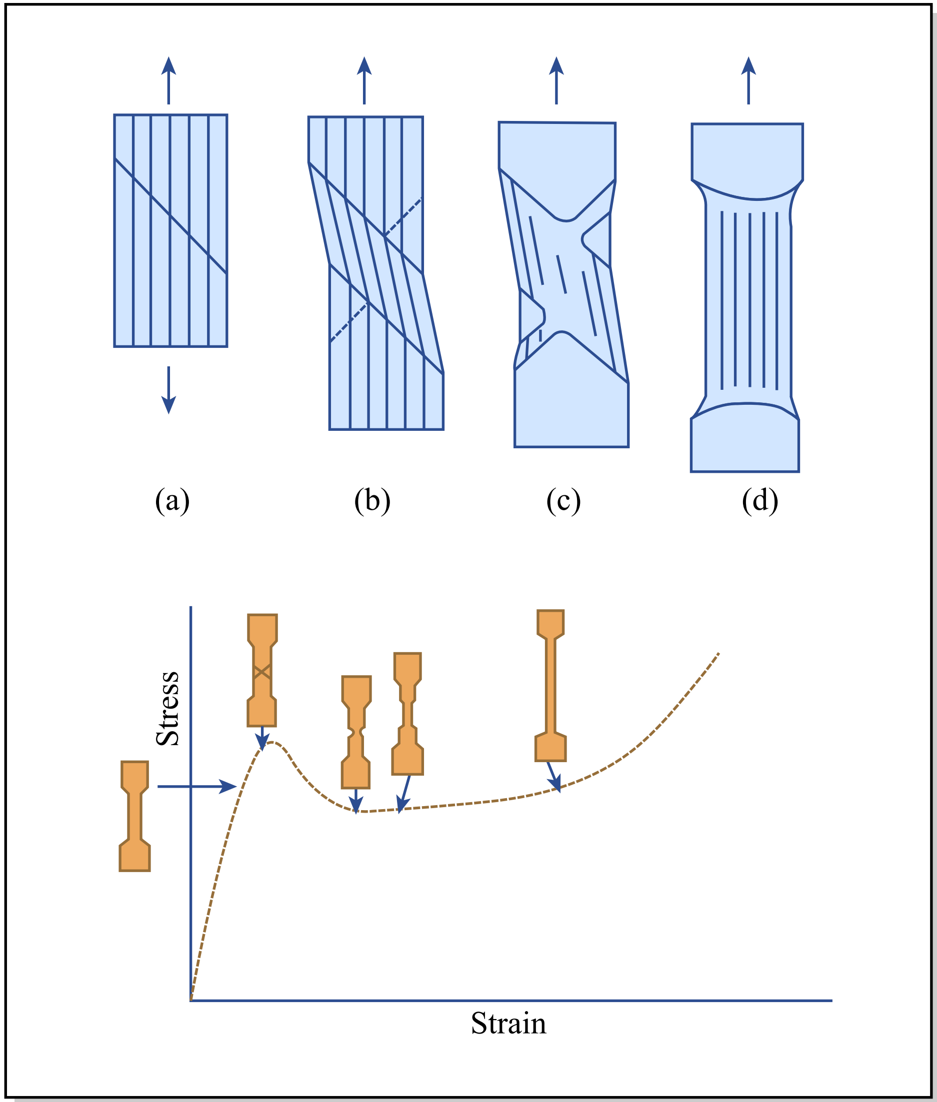

Figure by MIT OCW.

Shear banding in tension or compression.

Neck formation via shear bands

Image removed due to copyright restrictions.

Please see Fig. 12a and 15a in Shin, E., et al. “The Brittle-to-Ductile Transition in Microlayer Composites.” *Journal of Applied Polymer Science* 47 (1993): 269-288.

MicroShear Bands

Strain Rate Dependence

Yield stress increases as strain rate increases

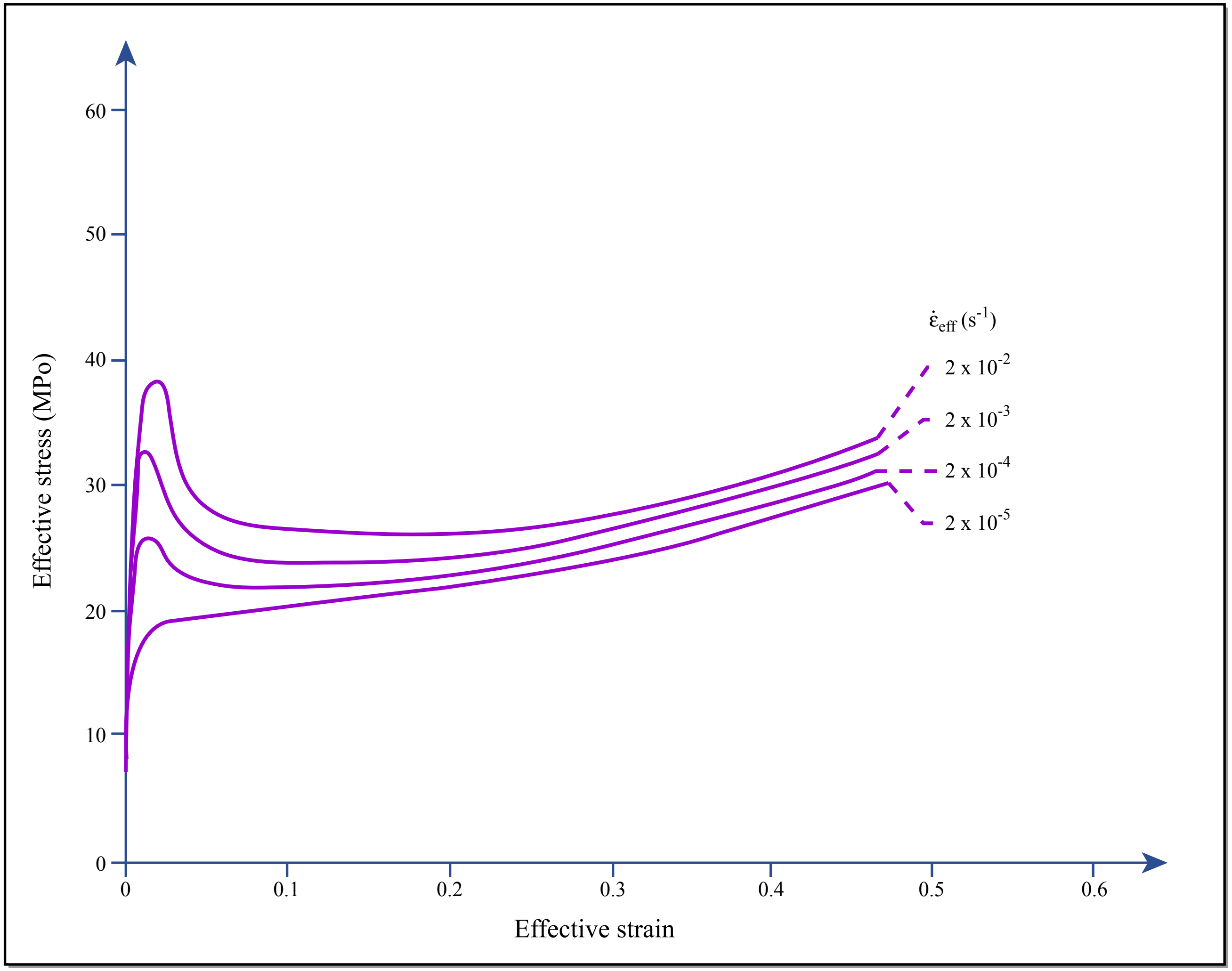

Figure by MIT OCW.

Polycarbonate @ 125 C

Temperature Dependence

Modulus and Yield Stress increase with decreasing T

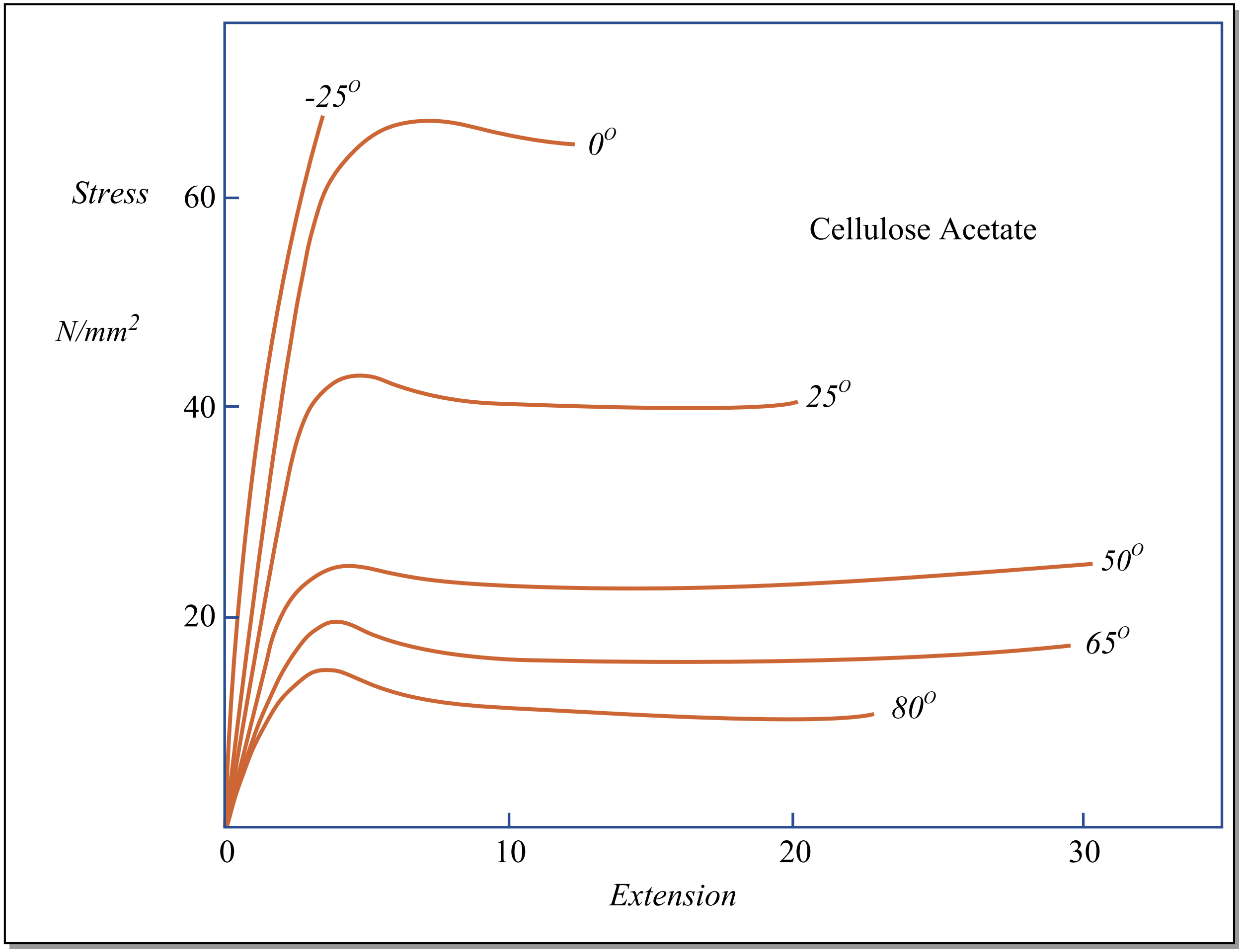

Figure by MIT OCW.

Molecular Theories of Localized Flow in Glassy Polymers

$$Eyring\ \ Theory\ \ of\ \ Viscous\ \ Flow$$

$$\upsilon_o \ = \ B \ e^{-\Delta G^* /kT}$$

$$Apply \ \ shear \ \ stress \ \ \sigma$$

$$\upsilon_f \ = B \ e^{-(\Delta G^* \ - \ .5\sigma Ax)/kT}$$

$$\upsilon_f \ = \ \upsilon_o \, e^{(\sigma Ax)/2kT}$$

$$\upsilon_b \ = \ \upsilon_o \, e^{-(\sigma Ax)/2kT}$$

$$strain \ \ rate \ \ d\varepsilon/dt \ \ is \ \ proportional \ \ to \ \ \upsilon_f \ - \ \upsilon_b$$

$$de/dt \ = \ \upsilon_o \, e^{(\sigma Ax)/2kT} \ - \ \upsilon_o \, e^{-(\sigma Ax)/2kT} \ = K \ \sinh \frac{\sigma V}{2kT}$$

$$where \ \ V \ = \ Ax \ = Activation \ \ volume$$

Pressure Dependence of Yield Stress

P = 1/3 (sum of 3 principal stresses)

Strain rate 7 x 10^{-3} sec -1 @ 25 C

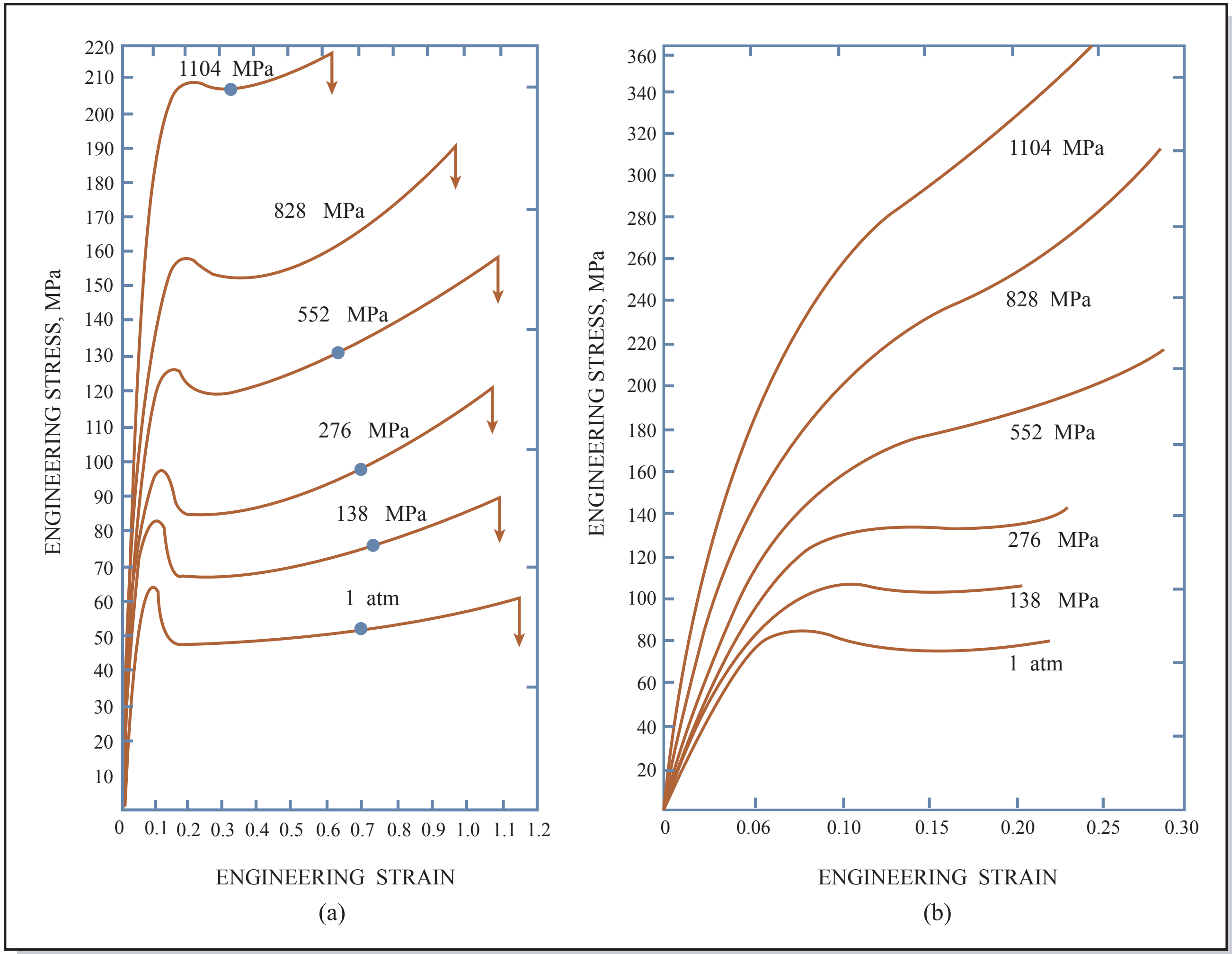

Figure by MIT OCW.

Polycarbonate

Crazes in Amorphous Glassy Polymers

Crazing in tension only,
not in compression.

Image removed due to copyright restrictions.

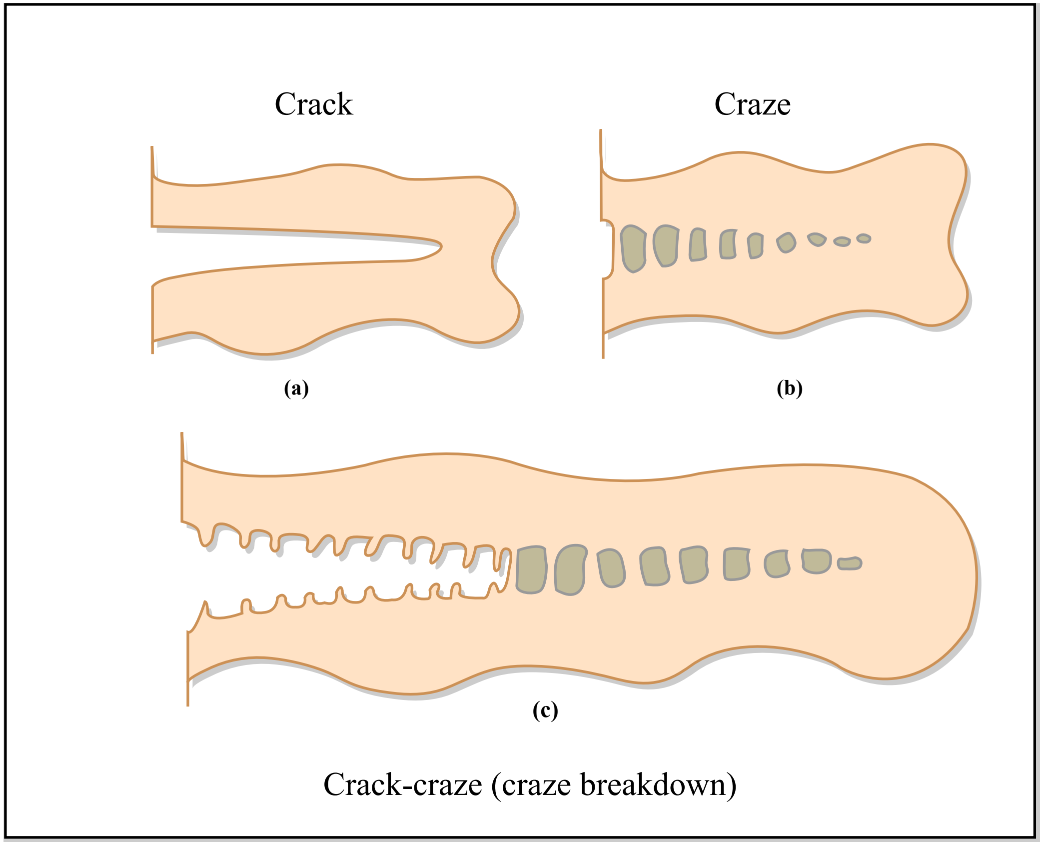

Figure by MIT OCW.

Crazes extending across PC tensile specimen

Designs: 12-Connected Stretch Dominated Structures

Octo-Truss Structure

(Red Curves)

Inverse FR-D IL Structure

(Blue Curves)

Please see: Fig. 3 in Maldovan, Martin, et al. "Sub-Micrometer Scale Periodic Porous Cellular Surfaces: Microframes Produced by Holographic Interference Lithography." *Advanced Materials* 19 (2007): 3809-3813.

Experimental Realization and FEM (linear) of P Microframe

6-connected

Single P

Tubular P

Images removed due to copyright restrictions.
Please see: Fig. 4 in Maldovan, Martin, et al. "Sub-Micrometer Scale Periodic Porous Cellular Surfaces: Microframes Produced by Holographic Interference Lithography." *Advanced Materials* 19 (2007): 3809-3813.

Single P (0.21 to 0.79)

Tubular P (solid line) , Single P (Dots)

3D Microframe with 200 nm feature size - Large Strain Deformation

Images removed due to copyright restrictions.

Please see Fig. 1c, d, e in Jang, J.H., Ullal, C.K., Choi, T., LeMieux, M.C., Tsukruk, V.V., Thomas, E.L. "3D Polymer Microframes that Exploit Length-Scale Dependent Mechanical Behavior." *Advanced Materials* 18 (2006): 2123-2127.

- **L/D ~ 3.2 for struts**
  ~ 2.3 for posts

- **Density ~ 0.3 gm/cm^3**

Large Strain Deformation Modes of Microframe

Images removed due to copyright restrictions.

Please see Fig. 2b, c, 3b, c in Jang, J.H., Ullal, C.K., Choi, T., LeMieux, M.C., Tsukruk, V.V., Thomas, E.L. “3D Polymer Microframes that Exploit Length-Scale Dependent Mechanical Behavior.” *Advanced Materials* 18 (2006): 2123-2127.

Mechanical Properties of SU8

1. SU-8: negative photoresist; used in MEMS applications.

Tensile test results of 130 μm SU-8 film:

Bulk

Image removed due to copyright restrictions.

Please see Fig. 2 in Feng, Ru, and Farris, Richard J. “Influence of Processing Conditions on the Thermal and Mechanical Properties of SU8 Negative Photoresist Coatings.” *Journal of Micromechanics and Microengineering* 13 (2003): 80-88.

Feng & Farris (2003)

2. Abnormal mechanical behavior observed in SU-8 Microframe

NanoFrame

Image removed due to copyright restrictions.

Please see Fig. 3b in Jang, J.H., Ullal, C.K., Choi, T., LeMieux, M.C., Tsukruk, V.V., Thomas, E.L. “3D Polymer Microframes that Exploit Length-Scale Dependent Mechanical Behavior.” *Advanced Materials* 18 (2006): 2123-2127.

Ji-Hyun Jang *et al.* (2006)

Fabrication of SU-8 “fibers” using photolithography

1. Spin-coat SU-8 on Si substrates.

 (SU-8 2025: 25 μm, SU-8 2002: 2 μm, and SU-8 200.5: 0.5 μm)

2. Soft bake: 65 ^{o}C, 1 min; 95 ^{o}C 3 min.

3. Exposure: λ=365 nm; total dose: 270 mJ/cm^2.

 (A mask is an array of windows having a length of 1 mm and variable line widths of 25 μm, 2 μm, and 1 μm.)

4. Post-exposure bake: 65 ^{o}C, 1 min; 95 ^{o}C, 1 min.

5. Develop.

6. Hard bake: 180 ^{o}C 5 min.

Cross-sectional SEM images of the fibers:

Images of SU8 fibers removed due to copyright restrictions.

27 μm

20 μm

24 μm

1.6 μm

1.65 μm

0.5 μm

1 μm

Diameter:	25 μm	1.8 μm	0.7 μm

Get Simple: Tensile Behavior of SU8 "Fibers"

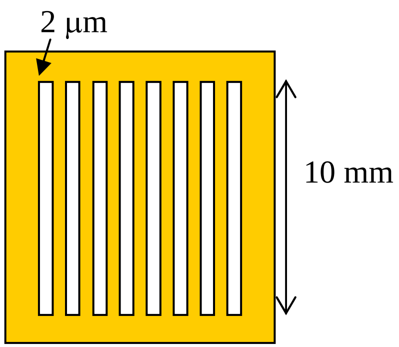

- Spin coat SU-8 on silicon substrates
- Soft bake: 65 ^oC, 1 min; 95 ^oC 3 min.
- Exposure: λ: 365 nm; total dose: 270 mJ/cm^2.
- Develop: SU-8 developer (from Microchem Corporation).
- Post-exposure bake: 65 ^oC, 1 min; 95 ^oC, 1 min.
- Hard bake: 180 ^oC 5 min.

Image of experimental apparatus removed due to copyright restrictions.

Cardboard template & fiber

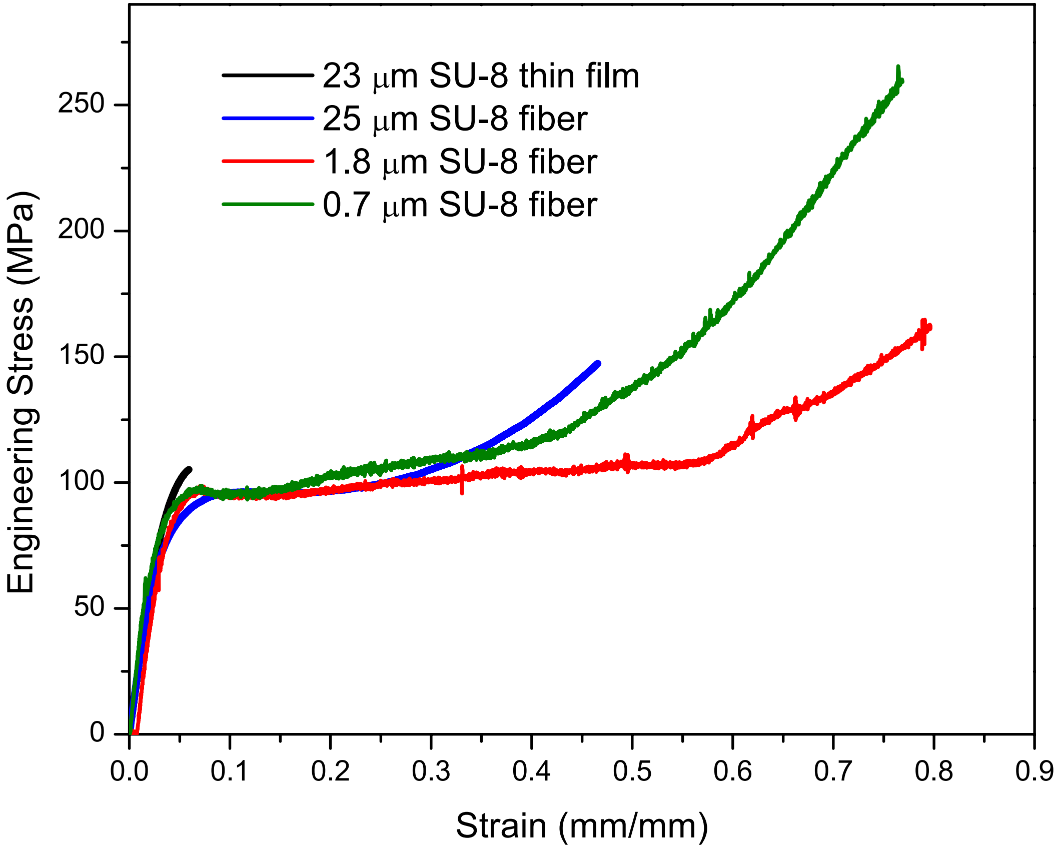

Tensile Test Results of SU-8 fibers

Without hard-baking

With hard-baking (180 ^{o}C, 5 min)

Stress-strain curves removed due to copyright restrictions.

Summary of SU8 Tensile Test Results

Toughness

Material	Kevlar	Polycarbonate	25 μm SU-8 fiber	1.8 μm SU-8 fiber	0.7 μm SU-8 fiber
Toughness (MPa)	120 ± 3.2	60	44 ± 0.5	72.5 ± 2.7	85.4 ± 3.3

Modulus

Plot of Young's modulus against fiber diameter removed due to copyright restrictions.

SU-8 film

Micromechanics of Tensile Deformation

Microscopic response under tension

Images of simulated deformation and stress-strain curve removed due to copyright restrictions.

Model

Actual Sample

Image removed due to copyright restrictions.

Please see Fig. 3b in Jang, J.H., Ullal, C.K., Choi, T., LeMieux, M.C., Tsukruk, V.V., Thomas, E.L. "3D Polymer Microframes that Exploit Length-Scale Dependent Mechanical Behavior." *Advanced Materials* 18 (2006): 2123-2127.

Lessons Learned

- Red indicates material deforming
- Blue indicates material not deforming
- Small scale of epoxy makes it deformable
- Micro-frame geometry creates multiple deformation domains which spread the deformation through the structure

Stress-Strain Behavior of Polygranular Isotropic Samples of 4 Microdomain Types

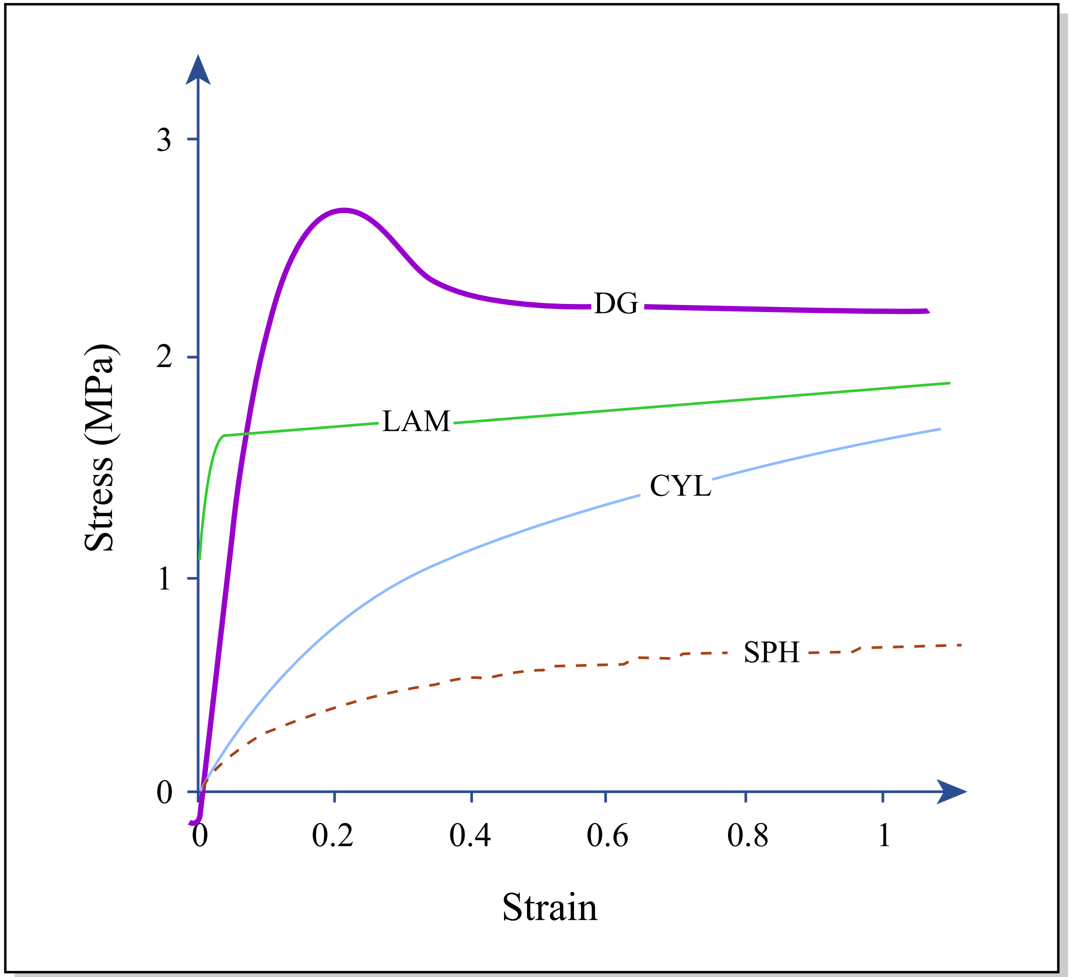

Figure by MIT OCW.

Roll-Casting of Block Copolymers

- Concept of roll-casting

X-Ray Diffraction Pattern and TEM Micrograph

Set-up of roll-caster

ABA Triblock Copolymer (Doped with Conjugated Polymer) with Cylindrical Morphology

- ⇨ Comercially available SIS block copolymer (M_n = 101,000 PDI = 1.05)
- ⇨ Films of block copolymers with nearly single crystal structure
- ⇨ Film Dimensions: 0.04mm Thick and 6 x 16 cm^2 in area

Deformation of Lamellar Morphology cont'd

Material:

Dexco Vector 4461-D

triblock copolymer

styrene-butadiene-styrene (18.5-45-18.5)

Roll-cast from 40% solution in toluene

Image removed due to copyright restrictions.

Please see Fig. 1 in Cohen, Yachin, et al. "Deformation of Oriented Lamellar Block Copolymer Films." *Macromolecules* 33 (2000): 6502-6516.

Deformation of Lamellar Microdomain Morphology

Image removed due to copyright restrictions.
Please see Fig. 4 in Cohen, Yachin, et al.
"Deformation of Oriented Lamellar Block
Copolymer Films." *Macromolecules* 33
(2000): 6502-6516.

SAXS

TEM

Roll cast lamellar BCP

Stress-strain Curves for Oriented Lamellar Films

Anisotropy

Image removed due to copyright restrictions.

Please see Fig. 2 in Cohen, Yachin, et al. “Deformation of Oriented Lamellar Block Copolymer Films.” *Macromolecules* 33 (2000): 6502-6516.

Perpendicular Deformation of Lamellae

In Situ SAXS X12B, NSLS, Brookhaven N.L.

At 20^{o}C

Image removed due to copyright restrictions.

Please see Fig. 5 in Cohen, Yachin, et al. "Deformation of Oriented Lamellar Block Copolymer Films." *Macromolecules* 33 (2000): 6502-6516.

Kinking Pattern

Image removed due to copyright restrictions.

Please see Fig. 8 in Cohen, Yachin, et al. “Deformation of Oriented Lamellar Block Copolymer Films.” *Macromolecules* 33 (2000): 6502-6516.

Model: The Lamellae Rotate in an Affine Relation to the Macroscopic Elongation

Image removed due to copyright restrictions.

Please see Fig. 17 in Cohen, Yachin, et al. "Deformation of Oriented Lamellar Block Copolymer Films." *Macromolecules* 33 (2000): 6502-6516.

Macroscopic measurement of elongation: $\lambda = L/L_o$

SAXS measurement of lamellar spacings: d_o and $d(\lambda)$

and rotation angle: α

Incompressibility: ad_o = constant

Affine rotation: $\lambda = L/L_o = d_+/d_o$

Affine Rotation Model

Predictions: $d(\lambda) = \text{constant} = d_o$

$\Rightarrow \lambda = 1/\cos\alpha$

In Situ SAXS Deformation

X12B, NSLS, Brookhaven N.L.

Test/confirm: d_o = 27nm, maintained throughout deformation
d at 600% strain (λ=5) is 25nm

SAXS - microscopic

Image removed due to copyright restrictions.

Please see Fig. 18 in Cohen, Yachin, et al. "Deformation of Oriented Lamellar Block Copolymer Films." *Macromolecules* 33 (2000): 6502-6516.

$1/\cos\alpha = \lambda$

Macroscopic

Parallel Deformation of Lamellae

(Note: very similar to cylinder parallel deformation)

Image removed due to copyright restrictions.

Please see Fig. 17 and 16 in Cohen, Yachin, et al. "Deformation of Oriented Lamellar Block Copolymer Films." *Macromolecules* 33 (2000): 6502-6516.